The string wave function across a Kasner singularity

Edmund J. Copeland[1*], Gustavo Niz[1†] and Neil Turok[2‡]

[1] *The School of Physics and Astronomy, University of Nottingham, University Park, Nottingham NG7 2RD, UK; and*

[2] *Perimeter Institute for Theoretical Physics, 31 Caroline St N, Waterloo, Ontario N2L2Y5, Canada.*

Abstract

A collision of orbifold planes in eleven dimensions has been proposed as an explanation of the hot big bang [1, 2, 10]. When the two planes are close to each other, the winding membranes become the lightest modes of the theory, and can be effectively described in terms of fundamental strings in a ten dimensional background. Near the brane collision, the eleven-dimensional metric is an Euclidean space times a 1+1-dimensional Milne universe. However, one may expect small perturbations to lead into a more general Kasner background. In this paper we extend the previous classical analysis of winding membranes to Kasner backgrounds, and using the Hamiltonian equations, solve for the wave function of loops with circular symmetry. The evolution across the singularity is regular, and explained in terms of the excitement of higher oscillation modes. We also show there is finite particle production and unitarity is preserved.

*ed.copeland@nottingham.ac.uk

†gustavo.niz@nottingham.ac.uk

‡nturok@perimeterinstitute.ca

1 Introduction

The initial singularity problem remains an open question in Cosmology and any model of the early Universe requires a resolution of this paradigm. We know general relativity breaks down close to it but there is hope that a theory of quantum gravity can resolve the singularity. Recently, interest has turned to the particular case of bouncing models, where the question of how information propagates across the big crunch/big bang transition has not been completely solved. For example, in the ekpyrotic/cyclic model this transition is assumed smooth with controlled particle production [1, 2]. In order to prove or disprove such a statement, most people have used effective field theories, constructed from string theory or other extensions of general relativity. There is plenty of literature on this approach to tackle the singularity problem (see for example [3]), however, most of these effective theories break down near the singularity, and perhaps one should be considering a more fundamental description beyond general relativity, such as string/M-theory. One such approach is to directly investigate the string equations of motion in a singular background [4], with special attention being given to the Milne universe [5, 6]. Some authors have used this to argue that this particular singularity can not be resolved [6], however, the results are not conclusive and in fact evidence from a dual description such as investigated in [7] seems to contradict the result. Furthermore, there is evidence that in a big crunch/big bang transition in asymptotically Anti de Sitter spacetime, the Conformal Field Theory (CFT) description leads to a well-defined evolution of fields across the singularity [8, 9]. In [10], the authors proposed a novel approach to explain the Milne singularity using eleven dimensional membranes, which is a natural setup for the cyclic universe, as also discussed recently in [11]. In this paper, we generalize this M-theory setup to more general backgrounds, corresponding to the homogeneous and anisotropic Kasner metrics. Such a background could well result once we include the effects of small perturbations in the background isotropic metric. Moreover, we also make progress in the quantum evolution of such membranes across the singularity.

In the M-theory model of [10], the singularity is described by two orbifold planes that collide as the eleventh dimension, which separates them, disappears. The study focuses on the evolution of membranes stretching from one orbifold plane to the other, but in particular, considers winding membranes, which correspond to the lowest Kaluza Klein modes in ten dimensions. As argued in [10], the winding membranes represent the lightest modes and decouple from the bulk (heavy Kaluza Klein) modes when the eleventh dimension is sufficiently small. From the ten dimensional point of view, these winding membranes are described by perturbative string theory, hence they include perturbative gravity. The classical evolution has been studied in the case of the Milne universe [13], and some progress has been made to understand the quantum theory of such modes, either by taking semiclassical approximations, such as the instanton calculations of [10] or by prescriptions to linearize the classical equations of motion, as in [13]. Furthermore, as shown in [14] the classical evolution does not acquire finite-width α'-corrections either far away from the singularity or very close to it. Therefore, on either side of the singularity there are two semiclassical regimes connected by a phase where quantum corrections are important. In the present analysis the story repeats, but in this case we quantize the action for certain membranes – corresponding to circular

strings from the ten dimensional theory – and show how particle production remains finite even though higher oscillation modes are excited.

In the ekpyrotic/cyclic universe, the spacetime is well described by the Milne universe near the orbifold collision [1, 2]. However, it is well known that as the singularity is approached, any small perturbation to the Milne universe can lead to a Kasner solution (see for example [12]). Therefore, we believe it is important to show how these winding membrane modes evolve across Kasner metrics. The metric, $g_{\mu\nu}$, for an eleven dimensional Kasner space-time is given by

$$ds_{11}^2 = -dt^2 + \sum_{i=1}^{10} |\theta_0 t|^{2p_i} (dx^i)^2, \tag{1}$$

where θ_0 is a dimensionful positive constant, which for the eleventh direction represents the rapidity at which the two orbifold planes collide. The usual Kasner conditions hold in eleven dimensions:

$$\sum_{i=1}^{10} p_i^2 = 1 = \sum_{i=1}^{10} p_i. \tag{2}$$

We have chosen the singularity to be at $t = 0$ and we have glued the manifolds before and after the singularity using the absolute-value function. In general, $t = 0$ is a curvature singularity, and only for the particular case of $p_i = 1$ for a given coordinate, does the solution become a direct product of a 9d flat space-time and the Milne universe, with $t = 0$ a coordinate singularity, which simply represents the fact that we have made a bad choice of coordinates in flat space. However, if the spatial coordinate of the Milne metric is compact, then the singularity is a conical singularity. This is the case of the cyclic universe where the big crunch/big bang transition is modeled by an orbifold collision, where the eleventh dimension is compact with a Z_2 symmetry. The orbifold structure is not essential for the present discussion, because our results only rely on a very small compact eleventh dimension, so we will forget about this discrete symmetry. In other words, because we are concentrating only on the Bosonic sector of the theory, where all the string models have the same field content, our results apply to either Heterotic or IIA limit of M-theory.

When the eleventh dimension, x^{10}, is small enough we can use a ten dimensional description based on the Kaluza-Klein reduction

$$ds_{11}^2 = e^{-2\phi/3} ds_{10}^2 + e^{4\phi/3} d(x^{10})^2, \tag{3}$$

where the dilaton is given by $\phi = \frac{3}{2} p_\phi \ln |\theta_0 t|$ (with $p_{10} \equiv p_\phi$), and the ten dimensional metric reduces to

$$ds_{10}^2 = a(t)^2 ds_{conf}^2 = a(t)^2 \left(-dt^2 + \sum_{i=1}^{9} |\theta_0 t|^{2p_i} (dx^i)^2 \right), \qquad a(t) = |\theta_0 t|^{p_\phi/2}, \tag{4}$$

where we have assumed $p_\phi > 0$, implying the eleventh dimensions disappears as $t \to 0$. As $x^{10} \to 0$ we can think of these winding membranes as fundamental strings on the orbifold planes feeling the metric (4). Alternatively, the winding membranes can be thought of as

strings with a time-dependent tension living on the metric ds^2_{conf}, as will become evident later. Since the string coupling is e^{ϕ}, for really small times — close to the singularity — the strings hardly interact and one can take the free string action as a good description. Therefore, we will focus our attention on the propagation of free strings on the ten dimensional dilaton-Kasner background (4).

The paper is organized as follows: in Section 2, we write down the different actions for membrane excitations in eleven dimensions, and in the following section we solve the classical equations of motion governing only winding membranes with cylindrical symmetry. Section 3 is devoted to the quantum description of circular loops using a Hamiltonian approach, before we finally conclude in Section 4.

2 Winding membranes

Our starting point is a Polyakov type of action for a bosonic membrane of tension μ_2 in eleven dimensions

$$S_{pol} = -\frac{\mu_2}{2}\int d^3\sigma \mathcal{L}_{pol} \tag{5}$$

$$= -\frac{\mu_2}{2}\int d^3\sigma \sqrt{-\gamma}\left(\gamma^{\alpha\beta}\partial_\alpha x^\mu \partial_\beta x^\nu g_{\mu\nu} - 1\right), \tag{6}$$

where x^μ are fields representing the position of the membrane in a target space with metric $g_{\mu\nu}$. The worldvolume spanned by the coordinates σ^α has a metric $\gamma_{\alpha\beta}$, and the variation of this action with respect to $\gamma_{\alpha\beta}$ yields the constraint $\gamma_{\alpha\beta} = \partial_\alpha x^\mu \partial_\beta x^\nu g_{\mu\nu}$, which can be substituted back into the action to obtain the Nambu-Goto action,

$$S_{NG} = -\mu_2 \int \mathrm{d}^3\sigma \sqrt{-\mathrm{Det}(\partial_\alpha x^\mu \partial_\beta x^\nu g_{\mu\nu})}. \tag{7}$$

The first action is more convenient to analyze the quantum behavior whereas the second is more useful to describe the classical evolution, as we will show below. As explained in [10], the Hamiltonian can be constructed from the action (6), leading to the constraints

$$\mathcal{H} \equiv \pi_\mu \pi_\nu g^{\mu\nu} + \mu_2^2 \mathrm{Det}(\partial_{\hat{\alpha}} x^\mu \partial_{\hat{\beta}} x^\nu g_{\mu\nu}) = 0, \qquad \mathcal{P}_{\hat{\alpha}} \equiv \pi_\mu \partial_{\hat{\alpha}} x^\mu = 0, \tag{8}$$

where $\pi_\mu \equiv \frac{\partial \mathcal{L}_{pol}}{\partial \dot{x}^\mu}$ are the canonical conjugate momenta to x^μ, $\dot{x}^\mu \equiv \frac{\partial x^\mu}{\partial \sigma^0}$ and the hatted indices run over the spatial dimensions of the membrane's worldvolume. Therefore, the most general Hamiltonian is

$$H = \int d^2\sigma \left(\frac{A}{2}\mathcal{H} + A^{\hat{\alpha}}\mathcal{P}_{\hat{\alpha}}\right), \tag{9}$$

where the two functions A and $A^{\hat{\alpha}}$ represent the gauge freedom of the membrane's metric diffeomorphisms. We consider a partial gauge where the momentum is always orthogonal to the membrane, which is equivalent to choosing $A^{\hat{\alpha}} = 0$, and will use the remaining gauge

freedom to simplify the equations of motion and obtain either classical or quantum solutions. A winding membrane is obtained by demanding its coordinates x^μ are independent of one of the spatial membrane worldvolume coordinates (say σ^2), except for the eleventh dimension which should be proportional to σ^2. We choose $x^{10} = \sigma^2$ (where σ^2 runs from 0 to 1), so that after integrating with respect to σ^2 in (7) we get an overall factor of $|\theta_0 t|^{p_\phi}$ in front of the effective string action.

3 Classical evolution

To describe the classical evolution of a winding membrane in a Kasner background we use the $t = \tau$ gauge in the Nambu-Goto type of action (7). Then the action reduces to

$$S = -\mu_2 \int d\sigma d\tau |\theta_0 t|^{p_\phi} \sqrt{\left(1 - \sum_{i=1}^{9} |\theta_0 t|^{2p_i} (\dot{x}^i)^2\right) \sum_{i=1}^{9} |\theta_0 t|^{2p_i} (\partial_\sigma x^i)^2}, \tag{10}$$

where $\tau \equiv \sigma^0$ and $\sigma \equiv \sigma^1$. For simplicity we will assume $\theta_0 = 1$ during the calculations and then restore a general θ_0 at the end. The equations of motion, in units of $\mu_2 = 1$, read

$$\begin{aligned} \dot{x}^i &= \frac{\pi_i |t|^{-2p_i}}{\epsilon}, & \dot{\pi}_i &= |t|^{2(p_\phi + p_i)} \partial_\sigma \left(\frac{\partial_\sigma x^i}{\epsilon}\right), \\ \dot{\epsilon}_i &= (p_\phi + 2p_i)|t|^{2(p_\phi+2p_i)} \frac{(\partial_\sigma x^i)^2}{t\,\epsilon_i}, & \epsilon_i^2 &= \pi_i^2 + |t|^{2(p_\phi+2p_i)} (\partial_\sigma x^i)^2, \end{aligned} \tag{11}$$

where the string energy density $\pi_0 \equiv \epsilon$ is given by

$$\epsilon^2 = \sum_{i=1}^{9} |t|^{-2p_i} \epsilon_i^2. \tag{12}$$

Using the last expression we can rewrite the differential equation for ϵ_i in the following way

$$\partial_t \left(\frac{\epsilon_i^2}{|t|^{2(p_\phi+2p_i)}}\right) = -\frac{2(p_\phi + 2p_i)}{t|t|^{2(p_\phi+2p_i)}} \pi_i^2, \tag{13}$$

which will be useful later. From (11), divergent solutions arise when at least one of the Kasner exponents in the 10d space-time is negative enough to lead to a divergent term in the energy density ϵ at $t = 0$, as previously shown by Tolley [15]. On the other hand, regular solutions across $t = 0$ are obtained if all $p_i \geq -p_\phi/2$. To avoid divergences we will assume

$$p_i \geq -p_\phi/2 \qquad \text{for all } i. \tag{14}$$

The divergent cases correspond to situations where, before the singularity, one spatial dimension expands faster than the contraction of the 10d conformal factor $a(t)$, as appreciated in (4). We are more interested in situations which are small perturbations away from the Milne universe, but still close to it.

To construct a perturbative solution around the singularity, one can expand the equations of motion (11) in terms of the string tension, as was done in [13]. Formally, one introduces a parameter λ in place of the tension (i.e. $\mu \to \mu\lambda$) and solves iteratively the equations of motion as a series in λ. At the end, one sets $\lambda = 1$. As shown in [13], the only equation where λ appears is $\dot{\pi}_i = \lambda |t|^{2(p_\phi + p_i)} \partial_\sigma \left(\frac{\partial_\sigma x^i}{\epsilon} \right)$, whose solution to zeroth order in λ is $\pi_i = \pi_i(0)$, where $\pi_i(0) = \pi_i(0, \sigma)$ is the loop momentum at $t = 0$. Assuming (14) holds, one can integrate equation (13) and insert the solution of ϵ and π_i in the $\dot{x}_i$-equation, to obtain the zeroth order solution

$$x^i(t) \simeq x^i(0) + \int_{t_0}^{t} dt \frac{\pi_i(0) |t|^{-2p_i}}{\sqrt{\sum_j |t|^{-2p_j} \left[\pi_j^2(0) + (\partial_\sigma x^j(0))^2 \, |t|^{2p_\phi + 4p_j} \right]}} + \mathcal{O}(\lambda), \tag{15}$$

where $x^i(0) = x^i(0, \sigma)$ is the string shape at the singularity. The last integral is finite, hence the solution is regular at $t = 0$. In general, this integral has to be done numerically, but there are specific string geometries or configurations where the solution can be found analytically; this is the case of a circular string.

3.1 Circular loops

For the rest of the paper we will focus on the circular loop, which as explained in [13] is the classical analogue of the dilaton field. The simplification rests on the fact that the only dynamical coordinate is the radius of the circle. Furthermore, to preserve the circular symmetry, the two Kasner exponents of the plane where the loop oscillates should be equal. Without loss of generality, we assume the circular loop oscillates in the xy plane and has a center of mass velocity v in the z direction, with the ansatz $x^i = (R(t)\cos(\sigma), R(t)\sin(\sigma), v\tau, 0, ..., 0)$, and the Kasner exponents in these directions are $p \equiv p_1 = p_2$ and $p_3 = p_z$. Under these assumptions the equations of motion (11) simplify to

$$\begin{aligned}
v &= \frac{\pi_z |t|^{-2p_z + p}}{\tilde{\epsilon}}, & \dot{\pi}_z &= 0, \\
\dot{R} &= \frac{\pi_R |t|^{-p}}{\tilde{\epsilon}}, & \dot{\pi}_R &= -|t|^{2p_\phi + 3p} \frac{R}{\tilde{\epsilon}}, \\
\dot{\tilde{\epsilon}} &= (p_\phi + 2p) |t|^{2(p_\phi + 2p)} \frac{R^2}{t\,\tilde{\epsilon}}, & \tilde{\epsilon}^2 &= \pi_R^2 + |t|^{2(p - p_z)} \pi_z^2 + |t|^{2(p_\phi + 2p)} R^2,
\end{aligned} \tag{16}$$

where $\pi_R^2 = \pi_1^2 + \pi_2^2$ and $\tilde{\epsilon} = t^p \epsilon$. Again, we can rewrite the differential equation for ϵ_i using the last constraint, namely

$$\partial_t \left(\frac{\tilde{\epsilon}^2}{|t|^{2(p_\phi + 2p)}} \right) = -\frac{2(p_\phi + 2p)}{t |t|^{2(p_\phi + 2p)}} (\pi_R^2 + |t|^{2(p - p_z)} \pi_z^2). \tag{17}$$

Moreover, in the case of a circular loop it is not hard to find another constraint by combining the different equations in (16), given by

$$(v^2 + \dot{R}^2) |t|^{2p} + \dot{\pi}_R^2 |t|^{-2(p_\phi + p)} = 1. \tag{18}$$

Notice that the speed (squared) of any point in the loop is $V^2 = V_z^2 + V_R^2 = (v^2 + \dot{R}^2)|t|^{2p}$, which is unaffected by the contraction or expansion of the plane of oscillation. After a careful analysis of the second term in the last constraint, one can be convinced that every point in the string reaches the speed of light ($V^2 \to 1$) as $t \to 0$, if the inequalities (14) hold. As a result of this, the solutions are not time invariant and the outgoing mode is different from the incoming one. Quantum mechanically this time asymmetry is the origin of particle production and excitation of higher order oscillation modes, as we will show later. This effect is enhanced when the center of mass momentum π_z vanishes. Furthermore, in the case when the bound (14) is saturated for the p Kasner exponent, the speed of the loop will be finite and generically smaller than the speed of light; hence there will not be a time asymmetry in the solution and no particle production or higher oscillation modes will be expected across the singularity. This should be expected, since the effective metric on the xy plane (see equation (4)) neither contracts or expands when the bound (14) is saturated for p.

Although the set of equations (16) can not be solved analytically everywhere they can be solved approximately in different regions and these results can then be compared to the full numerical solutions. The solutions evolve similarly to those in [13], so we refer the reader to this previous work for details. However, we would like to stress a few general points, especially when more general Kasner exponents are considered and not only the Milne case, as it was done in [13].

Far away from the singularity, the string does not feel the contraction or expansion of the universe, and therefore, it oscillates as if it lived in the ds^2_{conf} metric of equation (4), which reduces to flat spacetime for the Milne universe. Following the notation of [13], at a time t_0 the winding membrane in eleven dimensions can be effectively described by perturbative string theory in ten dimensions. Furthermore, the string coupling $e^{\phi} = |\theta_0 t|^{3p_\phi/2}$ tends to zero as the singularity is approached, hence the free string action becomes more accurate closer the orbifold collision. By definition, t_0 corresponds to the time where the string coupling hits unity, namely

$$t_0 = \theta_0^{-1}. \tag{19}$$

The string tension is therefore $\mu_1 = |\theta_0 t_0|^{p_\phi/2} = 1$ and its length is $l_s \sim \mu_1^{-1} = 1$. In terms of a quantum analysis we would expect this regime to be well described by a semiclassical solution, which can be obtained using the WKB approximation. However, classically we start with a string configuration in the metric ds^2_{conf} at time $t = -t_0$ and evolve it towards the singularity. The solution crosses the singularity and after it has reached a large enough positive time (comparable with $t = +t_0$), we can trust the description of strings living on the metric ds^2_{conf} again. We aim to compare both states, the ingoing and the outgoing states at $t = \pm t_0$ respectively, to determine whether there was particle production or excitation of higher vibrational states. Quantum mechanically, it corresponds to calculating a mini S-matrix, defined by the evolution of the quantum ingoing states at $t = -t_0$ to the outgoing ones at $t = +t_0$.

Starting from a large negative time in this adiabatic vacuum ($t = -t_0$), the string evolves into the singularity increasing its size, according to the contraction of the conformal factor of the universe. By a simple rescaling of the coordinates it is possible to show that the loop scales as a power of $1/a(t) \sim t^{-p_\phi/2}$. Once the size of the loop is comparable to the

averaged conformal Hubble radius ($\sim 1/|t|$), the "stringy" quantum corrections become really important and the evolution can no longer be described by a semiclassical analysis. Remember the string coupling goes to zero as $t \to 0$, hence only the α'-corrections become important as the solution approaches the singularity. As shown in [14], these α'-corrections modify the semiclassical evolution, but in a finite way. Finally, close to the singularity, there is another semiclassical phase in which the modes freeze, stop oscillating and cross the singularity. In detail, the string "breaks" into string bits which evolve independently of each other. In other words, the spatial gradients that tie the string together become negligible and the evolution only depends on time. This phenomenon is a consequence of the ultra-local behavior that one expects near a cosmological singularity (see for example [12]). At $t = 0$, however, the string receives an energy kick, because it has to travel at the speed of light, which either increases or decreases the amplitude of the outgoing mode, leading to classical gain or loss of energy. Quantum mechanically this translates into particle production, as we will discuss in the next Section.

Different Kasner exponents can dramatically change the outcome because they play an important role close to the singularity. In order to simplify the discussion, we will only consider the $\pi_z = 0$ case, but the analysis can be easily generalized for a non-zero center of mass momentum. Therefore, from the equations of motion (16) one may consider the exponents p and p_ϕ as two free parameters of the model, however, the 11d constraints (2) relate these parameters, together with the exponents of the orthogonal directions. To simplify the argument, one may think of the orthogonal exponents as being split into two sets, the first being all the same (m of them) and the other set being zero ($6-m$ of them), *i.e.* $p_i = \bar{p}$ ($i = 3, ..., m+3$) and $p_j = 0$ ($j = m+4, ..., 9$). Then, after solving for p_ϕ in terms of p and m using the constraints (2), one obtains

$$p_\phi = [(1-2p) \pm \sqrt{m(m+4p-2(m+3)p^2)}]/(m+1). \tag{20}$$

To get real exponents, p should lie between $(1-\sqrt{1+m(m+3)/2})/(m+3) \leq p \leq (1+\sqrt{1+m(m+3)/2})/(m+3)$. There is therefore a wider range of allowed values for p as m increases, but also divergent solutions are more likely to arise since p_ϕ may be smaller than $-2p$, and especially for the negative branch of the p_ϕ solution above (see Figure 1).

To have a feeling of how sensitive the solutions are to the Kasner exponents let us vary p around the Milne solution ($p = 0$ and $p_\phi = 1$). Figure (2) shows a slight variation around the Milne universe, and even though the general behavior remains similar, the amplitude and periodicity of the outgoing modes strongly depends on the precise value of the Kasner exponents. Figure (3) shows a more dramatic change near the singularity when the Kasner exponents are taken to be far away from the Milne universe. If $p \sim -p_\phi/2$, the energy density has a very mild dependence on $|t|$, so the modes do not feel the contraction or expansion of the universe. Therefore, there is no classical energy production, and as we will see later, there is also a mild particle production in the quantum theory, which consistently tends to zero for $p = -p_\phi/2$. The opposite case, when p is positive and relatively large, the string feels effectively a larger contraction/expansion of the scale factor, which produces a big effect around $t = 0$, and thus a greater quantum production of particles.

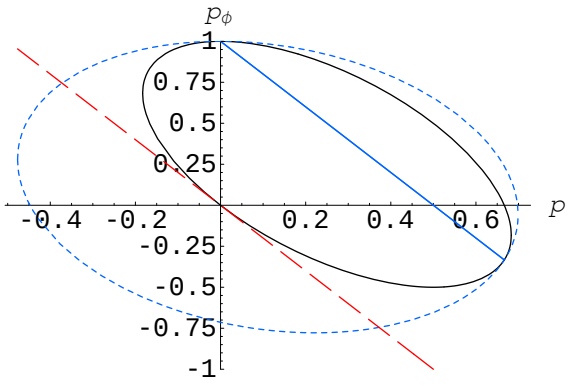

Figure 1: Kasner exponent p_ϕ as a function of the Kasner exponents in the xy plane (p) and the m equal-valued Kasner exponents in the orthogonal directions. The blue solid straight line is for $m = 0$, the solid line ellipsis is for $m = 1$ and the blue dotted one for $m = 6$. Divergent solutions which cannot be followed across the singularity correspond to values of p_ϕ below the red dashed line which only exist for $m > 1$.

As mentioned before, we can describe the evolution of these strings as an expansion in the string tension around $t = 0$. Formally, we introduce a parameter λ where the string tension is and then truncate the expressions to the desired order in λ. Finally we set $\lambda = 1$. This was done above explicitly for a general string configuration to zeroth order in the string coupling, and in the case of circular loop (with $\pi_z = 0$) the integral (15) can be solved analytically to give:

$$R = R_0 + t\,\frac{\mathrm{Sign}(\pi_R^0)}{(1-p)|t|^p}\;{}_2\mathrm{F}_1\!\left[\frac{1-p}{2(p_\phi+2p)},\frac{1}{2};1+\frac{1-p}{2(p_\phi+2p)};\frac{R_0^2}{\pi_R^0}|t|^{2(p_\phi+2p)}\right]+\mathcal{O}(\lambda), \tag{21}$$

where R_0 and π_R^0 are the values of R and π_R at $t = 0$, and ${}_2\mathrm{F}_1$ is the Gauss hypergeometric function, defined as the series

$${}_2\mathrm{F}_1[a,b;c;z] = \sum_{n=0}^{\infty}\frac{(a)_n(b)_n}{(c)_n n!}z^n, \tag{22}$$

with $(w)_n \equiv w(w+1)...(w+n-1)$ for any complex number w. The hypergeometric function is well behaved for all values of the Kasner exponents that satisfy the bound (14). Solution (21) reduces to that found in [13] for $p_\phi = 1$ (and $p = 0$).

4 Quantum description

We now turn our attention to the more complicated problem of quantization. If one tries to naïvely quantize the classical equations (11), all sorts of problems arise, because of the

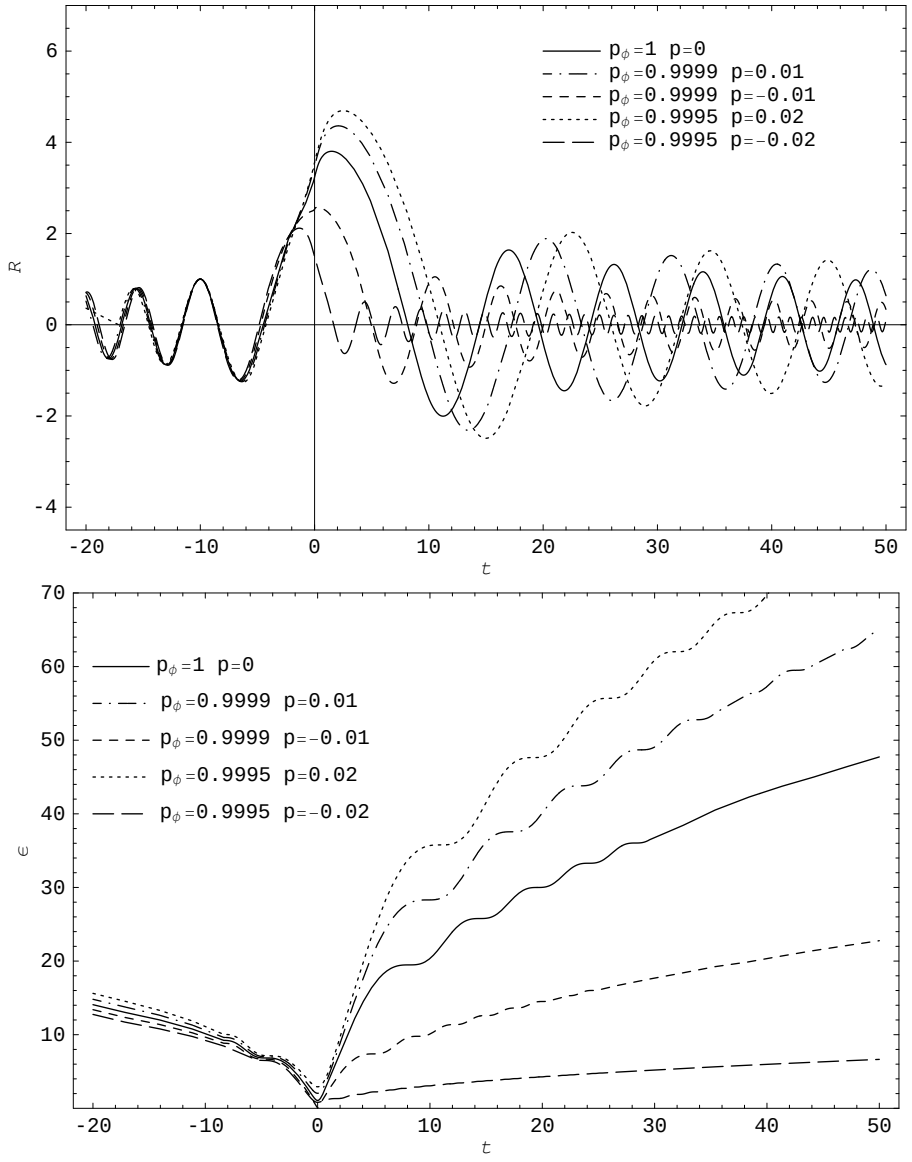

Figure 2: The radial coordinate R and the energy density $\tilde{\epsilon}$ evolving in time t for different Kasner exponents around the Milne solution ($p_\phi = 1$ and $p = 0$). The evolution is regular across $t = 0$, when the energy density takes its lowest value. The solutions are not time reversal and strongly depend on the Kasner exponents. We have assumed $\pi_z = 0$, and the initial conditions are $R(-t_0) = 1$ and $\dot{R}(-t_0) = 0$, with $t_0 = 20$.

square root present in the action. However, one can take a different approach, by considering the Polyakov type action and using the Wheeler-de Witt formalism, namely

$$\hat{H}\Psi = 0, \tag{23}$$

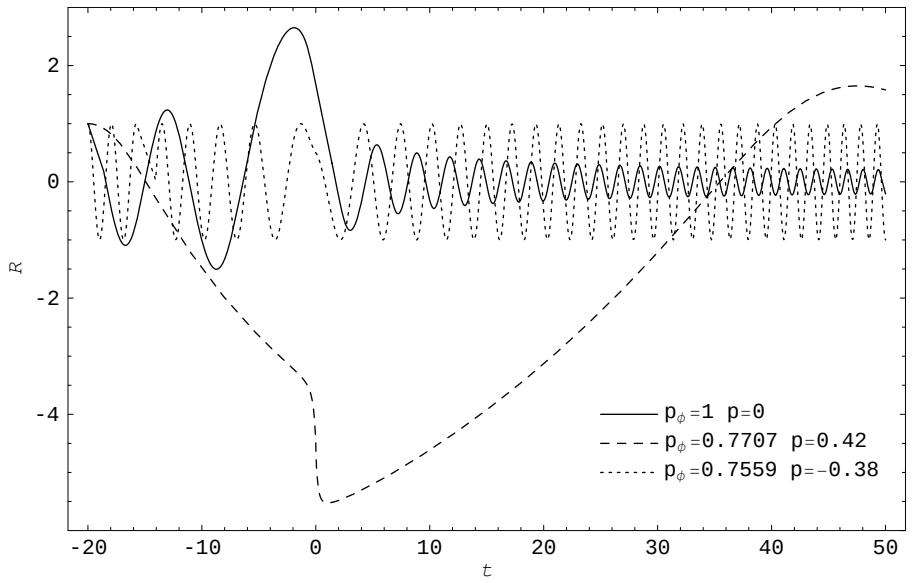

Figure 3: The radial coordinate R evolving in time t for different Kasner exponents far away from the Milne solution ($p_\phi = 1$ and $p = 0$). For positive p the kick around the singularity is stronger and the outgoing solution is drastically modified. On the other hand, negative values for p, close to saturating the bound (14), lead to relatively little modification of the outgoing solution, resulting in less particle production, as will be explained in the quantum model. We have assumed $\pi_z = 0$, and the initial conditions are $R(-t_0) = 1$ and $\dot{R}(-t_0) = 0$, with $t_0 = 20$.

where Ψ is the wave function of the string. However, it is hard to proceed from here, because the Hamiltonian includes a term proportional to $\partial_\sigma x^0 \equiv \partial_\sigma t$, so it is difficult to synchronize the different points on the string and to talk about a common time for the string. Fortunately, if we restrict ourselves to circular strings where the only degree of freedom is the radius of the loop, R, then the Hamiltonian simplifies enough for the problem to be tackled. In order to preserve the circular symmetry in time, we also need the Kasner exponents of the plane where the loop oscillates to be equal, as we assumed in the previous section. Moreover, a circular loop can have an initial center of mass momentum perpendicular to the plane of oscillation. We take the circular winding membrane ansatz $x^\mu = (t(\tau,\sigma^1), R(\tau)\cos(\sigma^1), R(\tau)\sin(\sigma^1), v\tau, 0, ..., 0, \sigma^2)$, where without loss of generality we allow the string to oscillate in the xy plane, with $p_1 = p_2 = p$, and a constant center of mass velocity v in the z direction with Kasner exponent $p_3 = p_z$. Notice that the circular symmetry forces $\partial_\sigma t = 0$, which implies t is a function of τ only. Then the Hamiltonian (9), reduces to

$$H = \int d^2\sigma \frac{A}{2}\left[-(\pi_0)^2 + |\theta_0 t|^{-2p}\pi_R^2 + |\theta_0 t|^{-2p_z}\pi_z^2 + |\theta_0 t|^{2(p_\phi+p)}R^2\right], \tag{24}$$

where, as mentioned before, we have chosen the partial gauge $A^{\hat{\alpha}} = 0$. To simplify this expression we can perform a canonical transformation to a new time coordinate given by $\tilde{t} \sim t^{1+p}$, up to a constant factor. Finally, because the Hamiltonian density does not depend on the spatial worldvolume variables, we can choose the extra gauge freedom to fix $A = 2t^{2p}/(\int d^2\sigma)$, simplifying the Hamiltonian to

$$H = -(\tilde{\pi}_0)^2 + \pi_R^2 + |\theta_0 \tilde{t}|^{2(\tilde{p}-\tilde{p}_z)} \pi_z^2 + |\theta_0 \tilde{t}|^{2(\tilde{p}_\phi + 2\tilde{p})} R^2, \tag{25}$$

where $\tilde{\pi}_0 = t^p \pi_0$ is the canonical momentum of $\tilde{t}$, and the new Kasner exponents are

$$\tilde{p}_\phi = p_\phi/(1+p), \qquad \tilde{p} = p/(1+p), \tag{26}$$

where we assume $p \neq -1$ (which is consistent with (14)). In fact, it is possible to rescale $\tilde{t}$ and R (preserving the Poisson brackets) in such a way that θ_0 only appears in the π_z term. Then, one can redefine the center of mass momentum to absorb the information of both, the orbifold rapidity θ_0 and the loop's center of mass momentum π_z, into a single parameter, π_o, in the following way

$$\pi_o = \theta_0^{(2\Delta p + s)/(s+2)} \pi_z, \tag{27}$$

where

$$s \equiv \tilde{p}_\phi + 2\tilde{p}, \qquad \Delta p \equiv \tilde{p} - \tilde{p}_z. \tag{28}$$

Notice that making θ_0 larger increases π_0 if $\Delta p > -s/2$, which is true within some open set of the allowed parameter space of the Kasner exponents. Evidently, this open set includes the Milne universe ($\tilde{p} = \tilde{p}_z = 0$ and $\tilde{p}_\phi = 1$). So in order to understand the physics of the cyclic model with respect to the orbifold rapidity, in what follows, we will consider Kasner combinations which obey $2\Delta p > -s/2$.

However, solutions of the wave function using the Hamiltonian (25) are messy when the term with π_0 is present, thus we will focus our attention to the limit $\pi_0 \to 0$ first and then present the results for a non-vanishing π_0. One can neglect π_0 in two different limits: either when the orbifold rapidity is very small compared to the loop's momentum, or when the center of mass velocity is small enough on its own[1].

4.1 Zero center of mass momentum

When dropping the center of mass momentum term, some observables, such as the amount of particle production, do not depend explicitly on the orbifold rapidity, which is given by θ_0. This statement may sound like a contradiction because we would expect more particles being produced for larger collision rapidities, but if one looks in more detail, the result is consistent with QFT in curved space. The basic idea of particle production is to measure the "difference" between two vacuum states, which in our case correspond to one in the far past, before the singularity, and another in the far future. However, a change in θ_0 not only

[1]Note that $\theta_0 < 1$ is needed to start with loops inside the Hubble horizon during the contracting phase, as shown in [13], so that in this case $\pi_z \simeq 0$ implies $\pi_0 \simeq 0$ (where we have also assumed $2\Delta p > -s/2$).

changes the orbifold rapidity but also the two vacua we are comparing, and for the case of $\pi_0 \to 0$ the changes are such that their effects cancel each other.

Therefore, knowing that we can absorb θ_0 by a constant rescaling of the variables in the case of negligible π_0, we will set $\theta_0 = 1$ and then restore it in the final expressions. Thus, for the present discussion we consider the simpler Hamiltonian

$$H = -(\tilde{\pi}_0)^2 + \pi_R^2 + |\tilde{t}|^{2s} R^2, \tag{29}$$

A canonical quantization ($\tilde{\pi}_0 \to i\partial_{\tilde{t}}$ and $\pi_R \to i\partial_R$) implies that the Wheeler-de Witt equation (23) reduces to

$$[\partial_t^2 - \partial_R^2 + |t|^{2s} R^2]\Psi(t, R) = 0, \tag{30}$$

where we have dropped the tilde over the time variable for simplicity, but the reader should remember that we are actually still referring to $\tilde{t}$ defined earlier. Eqn. (30) corresponds to the Klein-Gordon equation with the potential of a harmonic oscillator with a time-dependent frequency $\omega(t) \sim |t|^s$. There is a parallel line of thought to understand this result: as was mentioned earlier, an alternative description of a string evolving across the metric (4) is to think of a string oscillating in the space-time ds^2_{conf} with a tension that varies with respect to time (*i.e.* $\mu_1 = \mu_2 |\theta_0 t|^{p_\phi}$). From this point of view, a natural wave equation for the string is that of a harmonic oscillator in the metric ds^2_{conf} with a time-dependent mass, which after a change of variables can be recast into a time-dependent frequency problem (see for example [16]). Furthermore, when solving string equations in singular backgrounds, we generally find harmonic oscillator equations with a time-dependent frequency (see for example [17]).

4.1.1 Asymptotic solution

The first step to construct a solution to equation (30) is to understand the asymptotic behavior, where the adiabatic or WKB approximation provides a good approximation to the true solution. Naïvely we would expect this to be in the adiabatic regime when $|t|$ is large enough, however, as we will see later, the story is a bit more complicated and the adiabatic regime holds only for large T time ($T \sim t^{(2+s)/2}$) [2]. Nevertheless, we can still get a feeling of the asymptotic solution if we set the frequency to be constant, namely

$$[\partial_t^2 - \partial_R^2 + t_0^{2s} R^2]\Psi(t, R) = 0, \tag{31}$$

where $t_0 >> 1$. The wave function that solves this simplified equation is related to the usual harmonic oscillator form, and is given by

$$\Psi(t, R) = \sum_{n=0}^{\infty} H_n(t_0^{s/2} R) \exp(-t_0^s R^2/2) \left[A \exp(iE_n t) + B \exp(-iE_n t)\right], \tag{32}$$

where $E_n^2 \equiv (2n+1)t_0^s = (2n+1)\omega(t)$ and $H_n(x)$ is the Hermite polynomial of degree n. Notice that the energy levels E_n are actually the square root of the usual harmonic oscillator

[2] Remember the effective (2+1)-metric where the string oscillates is given by equation (4), namely $ds^2_{3d} = |t|^{p_\phi}(-dt^2 + |t|^{2p} dx^2 + |t|^{2p} dy^2) = |\tilde{t}|^{(\tilde{p}_\phi + 2\tilde{p})}(-d\tilde{t}^2 + dx^2 + dy^2)$, where $\tilde{t} \sim t^{p+1}$ and $\tilde{p}_\phi$ and $\tilde{p}$ given by (26). Therefore, the "10-dimensional" time T is simply given by $T = \int dT \sim \int \tilde{t}^{s/2} d\tilde{t}$, with $s = \tilde{p}_\phi + 2\tilde{p}$.

levels. To understand this, one can think of the classical string analysis previously done, where in fact, the Hamiltonian $\tilde{\epsilon}$ (see equation (16)) is the square root of the harmonic oscillator for constant time.

The asymptotic solution (32), provides a hint as to the best ansatz we can adopt to obtain the general solution to (30). Using the harmonic oscillator as a basis and replacing t_0 by t, we consider an ansatz of the form:

$$\Psi(t,R) = \sum_{n=0}^{\infty} A_n(t) H_n(|t|^{s/2}R) \exp(-|t|^s R^2/2), \tag{33}$$

where the A_n's are considered to be functions of time and determine the evolution of the harmonic oscillator states from the incoming vacuum at negative times to the outgoing modes far after the singularity. We can then use the orthogonality of the Hermite polynomials

$$\int H_n(x) H_m(x) e^{-x^2/2} dx = \sqrt{\pi}(2^n n!)\delta_{mn} \tag{34}$$

and the relations $H_n'(x) = 2nH_{n-1}(x)$ and $H_{n+1}(x) = 2xH_n(x) - 2nH_{n-1}(x)$ to decompose equation (30) into an infinite system of coupled ODEs for the A_n's, which are given by the following recursive equation

$$\begin{aligned} 0 \;=\; & \ddot{A}_n - \frac{s}{2t}\dot{A}_n + \left[4s - s^2(1+2n+2n^2) + 16(1+2n)|t|^{2+s}\right]\frac{A_n}{16|t|^2} \\ & +(n+1)(n+2)\frac{s}{t}\dot{A}_{n+2} - (2+s)(n+1)(n+2)\frac{s}{4|t|^2}A_{n+2} - \frac{s}{4t}\dot{A}_{n-2} \\ & +(2+s)\frac{s}{16|t|^2}A_{n-2} + (n+1)(n+2)(n+3)(n+4)\frac{s^2}{4|t|^2}A_{n+4} + \frac{s^2}{64|t|^2}A_{n-4}. \end{aligned} \tag{35}$$

One should note that these equations are not regular at $t = 0$, so one cannot find solutions which interpolate between negative times and positives ones. This implies nothing else than using the harmonic oscillator basis is not a good approximation around the singularity. However, as we will see in the next section the evolution across the singularity is simpler than one could possibly have expected.

Consider the zeroth mode A_0 equation,

$$\ddot{A}_0 - \frac{s}{2t}\dot{A}_0 + \left(4s - s^2 + 16|t|^{2+s}\right)A_0 + \frac{2s}{t}\dot{A}_2 - \frac{s(2+s)}{2t^2}A_2 + \frac{6s^2}{t^2}A_4 = 0. \tag{36}$$

If we assume the higher modes are negligible, $A_n = 0$ for $n > 0$ (which should be the case if the incoming state is the vacuum and will be justified later), then Eqn. (36) can be solved in closed form for either positive or negative times, resulting in

$$A_0 = |t|^{(2+s)/4}(\theta_0)^{s/4}\left[c_1 K_l^{(1)}\left(2k\theta_0^{s/2}|t|^{(2+s)/2}\right) + c_2 K_l^{(2)}\left(2k\theta_0^{s/2}|t|^{(2+s)/2}\right)\right], \tag{37}$$

where $K_l^{(1)}(x)$ and $K_l^{(2)}(x)$ are the Hankel functions of the first and second kind respectively, c_1 and c_2 are integration constants, $k \equiv 1/(2+s)$, $l \equiv k\sqrt{1+s^2/2}$, and we have restored

θ_0 in the expression. Using the asymptotic expansion of the Hankel functions $K_\alpha^{(1,2)}(x) = \sqrt{\pi/(2x)}\exp\left(\pm i(x-(2\alpha\pm 1)\pi/4)\right)$, we obtain an asymptotic solution for the ground state given in terms of positive and negative frequency components, namely

$$\Psi(t,R) = exp(-|\theta_0 t|^s R^2/2)\left[C_1\exp(iE_0|t|) + C_2\exp(-iE_0|t|)\right], \tag{38}$$

where $C_1 = \sqrt{\frac{\pi}{2}}c_1\exp(-i(2\alpha+1)\pi/4)$, $C_2 = \sqrt{\frac{\pi}{2}}c_2\exp(i(2\alpha-1)\pi/4)$ and now the frequency is time-dependent and given by $E_0(t) = \sqrt{\omega_0(t)} = \frac{2}{2+s}|\theta_0 t|^{s/2}$.

To justify dropping the higher order modes (A_n with $n>0$) in equation (36) for large times one can re-write the recursive differential equation in terms of the T time ($T = \frac{2}{2+s}\theta^{s/2}t^{(2+s)/2}$) and then see which are the leading terms for large T. Equation (35), in T-time and with $\theta_0 = 1$, reads

$$0 = \frac{d^2A_n}{dT^2} + (1+2n)A_n + \mathcal{O}\left(\frac{1}{T}\right), \tag{39}$$

and has a large T solution,

$$A_n(t) = \exp(i\sqrt{2n+1}T) = \exp(iE_n t), \qquad E_n(t) = \frac{2\sqrt{2n+1}}{2+s}|t|^{s/2}. \tag{40}$$

The picture is then the following: asymptotically (large T), all the harmonic oscillator modes decouple from each other and as one approaches the singularity they start interacting. If one starts with the ground state as the incoming vacuum, then higher order modes become excited in order to resolve the singularity, and one ends up with a tower of states as the outgoing state in the far future, when again the interaction of harmonic oscillator modes stops and we can use this basis to describe the resulting state. Furthermore, since the A_n-equation (35) is a "double-step" recursive equation, if one starts with the ground state in the far past, then only even n-levels will be excited across the singularity.

4.1.2 Solution near the singularity

If we consider the vacuum positive energy mode (38) as the incoming state for $t\to -t_0$ (with $t_0 >> 1$), then we can evolve numerically the solution to the full equation (30). The numerical solution behaves regularly everywhere, particularly at $t=0$. In order to picture the evolution of the wave function across the singularity, we can use the integrated wave equation

$$\Psi(t) = \int_{-\infty}^{+\infty}\Psi(t,R)dR. \tag{41}$$

The numerical solution of such an integrated function is shown in Figure 4, and notice in particular that around $t=0$ the solution is simply given by a straight line, as we shall shortly describe. This result provides a simple explanation of how the modes evolve in terms of the absolute value function. The fact that the wave function (41) is well approximated by $\Psi(t) = at+b$ around $t=0$, can be understood as follows: assume Ψ behaves like

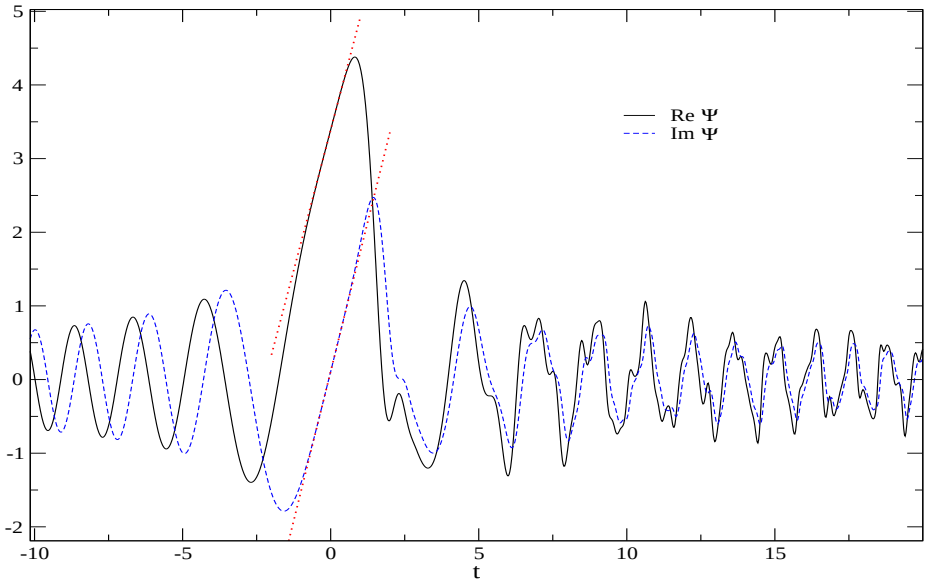

Figure 4: Evolution of the integrated wave function $\Psi(t)$ in time for the Kasner exponent combination $p_\phi = 0.793521$ and $p = 0.4$. The positive frequency mode in (38), with $C_1 = 1$ and $C_2 = 0$, at $t = -20$ was chosen. Different initial times do not change the behavior but the overall scale. Around $t = 0$ the wave function evolution follows a straight line, and after the singularity, higher order modes contribute to the overall wave function, leading to a non-periodic and complicated structure.

$\Psi(t, R) = e^{-|t|^s R^2/2} f(t)$ near the singularity[3]. After substituting it into the Hamiltonian equation (23), and assuming a simple polynomial function for $f(t)$ of the form $f(t) = at^m + c$, then the only solution with a well-defined limit as $t \to 0$ has $c = 0$ and $m = s/2,\ (2+s)/2$. Therefore, the solution near $t = 0$, which is valid on both sides of the singularity, is

$$\Psi(t, R) = e^{-|t|^s R^2/2}(at + b)|t|^{s/2}/\sqrt{2\pi}, \tag{42}$$

which after integrating over R implies $\Psi(t) = at + b$. If we think of the harmonic oscillator basis, the functions A_n should all behave as $(a_n t + b_n)|t|^{s/2}$ for small times on either side of the singularity. However, it doesn't mean we can simply solve for the individual coefficients a_n and b_n, because from (33) and (41) we require knowledge of all the modes that cross the singularity, thus no individual mode can be evolved across using this description for the integrated wave function around the singularity. Fortunately, from the numerical solution, we can always calculate the A_n coefficients using the orthogonally property (34) of the Hermite polynomials. Therefore, we can show the agreement between the numerical solution and the expected behavior ($(a_n t + b_n)|t|^{s/2}$). For example, Figure 5 shows the case of the zeroth mode A_0 before the singularity.

[3]If one plots the wave function near $t = 0$ as a function of R, one finds a good fit using the Gaussian profile $exp(-|t|R^2/2)$, which justifies our assumption.

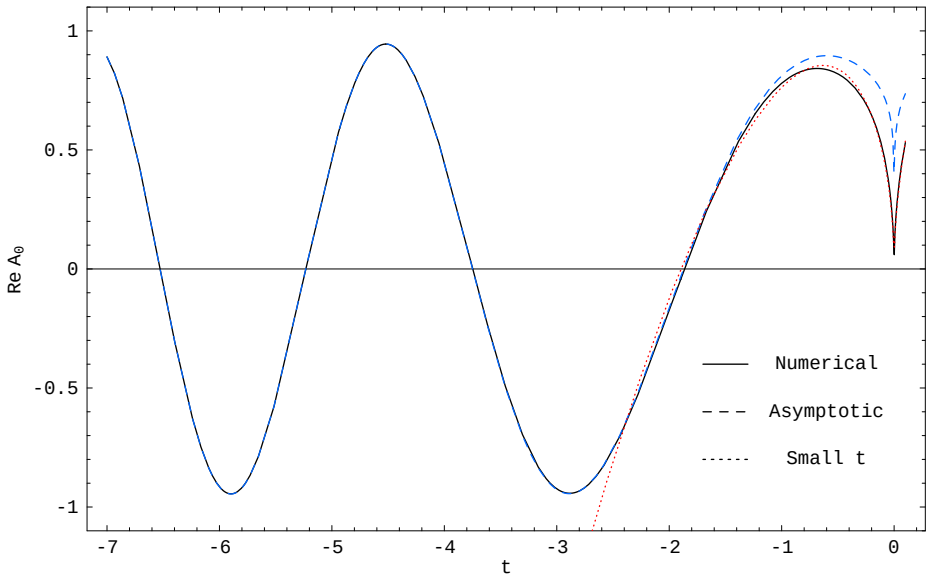

Figure 5: Using the orthogonality property (34) one can extract the coefficients of the harmonic oscillator modes A_n from the numerical solution of the wave function (see equation (33)). Here, we plot $Re(A_0)$ for $p_\phi = 1$ and $p = 0$. The dashed line represents the analytic solution (37) which follows the numerical solution (solid line) up to the place where the $t = 0$ behavior, given by solution (42) becomes more accurate (dotted line). We normalize the wave function so $A_0 \sim 1$ initially.

On the other hand, after $t = 0$ the R-integrated wave equation $\Psi(t)$ no longer looks periodic (see Figure 4). However, all of this complicated structure can be decomposed as a tower of higher harmonic oscillator modes, which were excited during the transition through $t = 0$ and converge as we increase the mode number (see Figure 6). The choice of Kasner exponents has an effect on the tower of excited states, as will be shown later when calculating the particle production.

Furthermore, if we follow the whole evolution of the vacuum state, the adiabatic regime is well approximated by the analytical solution (37), even as we approach the singularity. However, such an agreement inevitably breaks down very close to the singularity, as the expansion in terms of uncoupled harmonic oscillator states breaks down. That is, all higher modes begin to get excited in order to solve through the singularity, hence, we can not neglect the A_2 or A_4 terms in the A_0 equation near $t = 0$. However, notice that these higher order terms never dominate, as can be seen in Figure 6. As the adiabatic approach fails, the above mentioned polynomial behavior near $t = 0$ takes over and the solution can be followed all the way to and across the singularity. Some time after $t = 0$, the story repeats and we can use the adiabatic description again, leading to a decomposition of higher oscillation state, which can be described in terms of Bogoliubov transformations, as we will show in the following section.

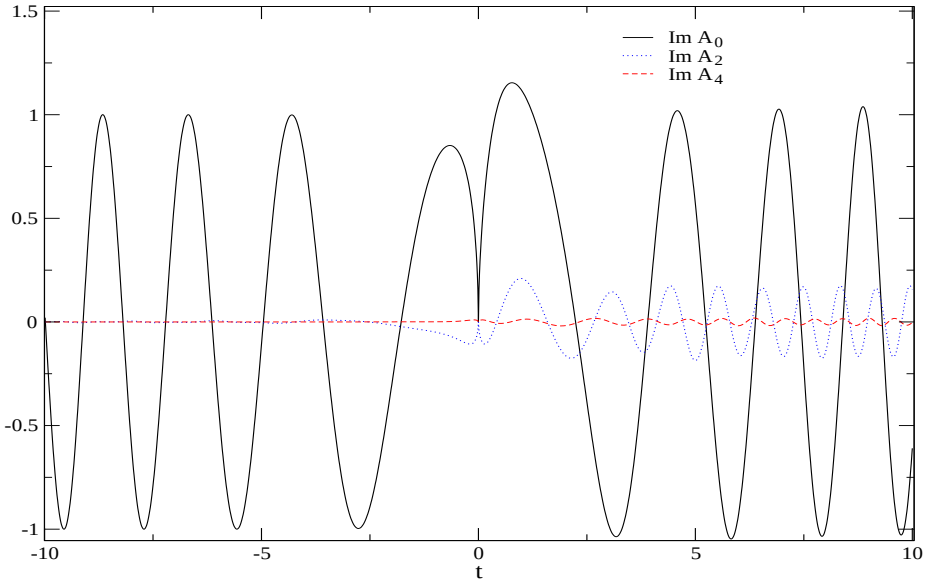

Figure 6: Using the orthogonality property (34) we plot the A_n's for different mode numbers n. One can see how higher modes get excited after $t = 0$, and the amplitude of higher states decrease with n as expected. We use $p_\phi = 0.793521$ and $p = 0.4$.

4.1.3 Particle production

One has to be careful when constructing the Hilbert space, since a C^∞ and globally hyperbolic manifold is needed. In our case the string metric is not well defined at $t = 0$, therefore we can split the space of solutions into two sections: for $t < 0$ and $t > 0$. Based on the regularity of the classical and quantum solutions around $t = 0$ it is natural to assume unitarity at $t = 0$, which allows us to use the Bogoliubov transformations to relate the two sections of the Hilbert space and calculate particle production. Our numerical results will act to justify this assumption. Moreover, a natural inner product in this Hilbert space is defined by [18]

$$(\Psi_1, \Psi_2) \equiv -i \int_\infty^\infty dR \left[\Psi_1 \frac{\partial \Psi_2^*}{\partial t} - \left(\frac{\partial \Psi_1}{\partial t} \right) \Psi_2^* \right]. \tag{43}$$

One can expand the wave function $\Psi(R, t)$ in terms of two basis sets, one for asymptotically negative times and one for the corresponding positive times, namely

$$\begin{aligned} \Psi(R,t) &= \sum_n a_n^{(in)} U_n^{(in)} + (a_n^{(in)})^\dagger (U_n^{(in)})^* \qquad t \to -\infty \\ &= \sum_n a_n^{(out)} U_n^{(out)} + (a_n^{(out)})^\dagger (U_n^{(out)})^* \qquad t \to +\infty \end{aligned} \tag{44}$$

where $a_n^\dagger$ and a_n are the creation and annihilation operators associated with the harmonic oscillator expansion, and which obey the usual commutation relationships (*i.e.* $[a_n, a_m^\dagger] =$

δ_{mn}, etc.). We would expect the negative time vacuum ($a_n^{(in)}|0\rangle_{in} = 0$) to be different from that of positive times ($a_n^{(out)}|0\rangle_{out} = 0$), leading to particle production. The functions $U_n^{(in)}$ and $U_n^{(out)}$ are the positive frequency modes

$$\begin{aligned} U_n^{(in)} &= \mathcal{N}_n \exp(+iE_n t)\exp(-|t|^s R^2/2) H_n(|t|^{s/2}R) \quad t<0, \\ U_n^{(out)} &= \mathcal{N}_n \exp(-iE_n t)\exp(-|t|^s R^2/2) H_n(|t|^{s/2}R) \quad t>0, \end{aligned} \tag{45}$$

with the normalization factor $\mathcal{N}_n$ given by

$$\mathcal{N}_n = (2^{n+1} n! \sqrt{(2n+1)\pi})^{-1/2}, \tag{46}$$

in such a way that $(\Psi_n, \Psi_m) = \delta_{nm}$.

Actually, since we are interested in having the vacuum as our incoming state, the wave function for $t \to -\infty$ takes the form

$$\Psi = \mathcal{N}_0 \left[\left(a_0^{(in)} + (a_0^{(in)})^\dagger \right) \cos(E_0|t|) - i \left(a_0^{(in)} - (a_0^{(in)})^\dagger \right) \sin(E_0|t|) \right] \exp(-|t|^s R^2/2), \tag{47}$$

where $\mathcal{N}_0 = \frac{1}{(4\pi)^{1/4}}$. Now, we can write explicitly the wave function for $t \to +\infty$ as

$$\begin{aligned} \Psi &= \sum_n \mathcal{N}_n \Big[\left(a_n^{(out)} + (a_n^{(out)})^\dagger \right) \cos(E_n t) - i \left(a_n^{(out)} - (a_n^{(out)})^\dagger \right) \sin(E_n t) \Big] H_n(t^{s/2}R) e^{-t^s R^2/2} \\ &= \sum_n \mathcal{N}_0 \Big[\left(a_0^{(in)} + (a_0^{(in)})^\dagger \right) \mathcal{D}_n \cos(E_0|t| + \varphi_n) \\ &\qquad - i \left(a_0^{(in)} - (a_0^{(in)})^\dagger \right) \bar{\mathcal{D}}_n \sin(E_0|t| + \bar{\varphi}_n) \Big] H_n(t^{s/2}R) e^{-t^s R^2/2}, \end{aligned} \tag{48}$$

where $\mathcal{D}_n$ and φ_n ($\bar{\mathcal{D}}_n$ and $\bar{\varphi}_n$) are the amplitude and phase — with respect to $t = 0$ — of the outgoing mode n after sending an incoming *cosine* (*sine*) piece of the incoming wave function (47). Since the two lines in the previous equation are equal, the coefficients should be related in the following way

$$a_n^{(out)} = \alpha_{n0}^* a_0^{(in)} + \beta_{n0}^* (a_0^{(in)})^\dagger, \tag{49}$$

where the Bogoliubov coefficients are defined as

$$\alpha_{n0} = \frac{\mathcal{N}_0}{2\mathcal{N}_n} \left(\mathcal{D}_n e^{i\varphi_n} + \bar{\mathcal{D}}_n e^{i\bar{\varphi}_n} \right), \qquad \beta_{n0} = \frac{\mathcal{N}_0}{2\mathcal{N}_n} \left(\mathcal{D}_n e^{i\varphi_n} - \bar{\mathcal{D}}_n e^{i\bar{\varphi}_n} \right). \tag{50}$$

Particle production at a given energy level can then be understood in terms of the expectation value of the particle number operator $\hat{N}_n = (a_n^{(in)})^\dagger a_n^{(in)}$ over the out-vacuum $|0\rangle_{out}$, which simplifies to the following

$$\langle 0|\hat{N}_n|0\rangle_{out} = \beta_{n0}\beta_{n0}^* = 2^{n-2} n! \sqrt{2n+1} \left(\mathcal{D}_n^2 + \bar{\mathcal{D}}_n^2 - \mathcal{D}_n \bar{\mathcal{D}}_n \cos(\varphi_n - \bar{\varphi}_n) \right). \tag{51}$$

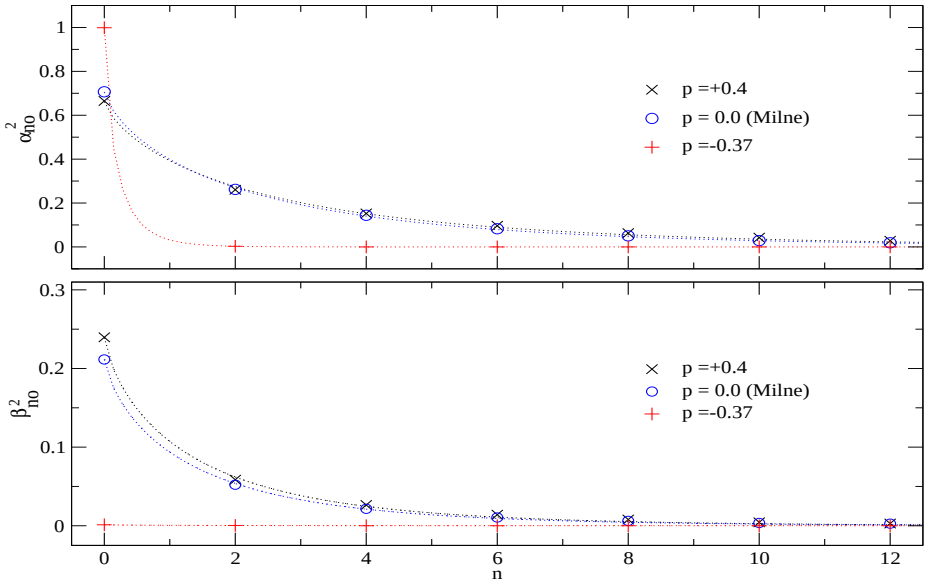

Figure 7: Bogoliubov coefficients α^2_{n0} and β^2_{n0} as functions of the mode number n for three Kasner exponent combinations: $p = 0.4$, $p = 0.0$ (Milne) and $p = -0.37$, with p_ϕ obtained using (20) for $m = 7$. In the last case, the effective (3+1)-metric where the string oscillates is almost flat, thus the particle production $|\beta|^2$ is negligible. A fit shows that both Bogoliubov coefficients decay as $C_1 \exp(-C_2 n^{3/4})$, where C_1 and C_2 are positive constants that depend on the Kasner exponents only.

Figure 7 shows the particle production for different Kasner exponents. A fit of this plot shows that the particle production decays exponentially with mode number, n, satisfying a fit of the form $\beta^2_{00} \exp(-C_1 n^{3/4})$, where β_{00} and C_1 depend on the particular choice of Kasner exponents. Of particular note is that for large n where the energy per mode, E_n satisfies $E_n^2 \sim n$, (see equation (40)), we then obtain an exponential decay of the form $\beta^2_{00} \exp(-C_1 E_n^{3/2})$, a result that agrees with the semiclassical instanton calculation in [10] for the Milne universe, but remains to be compared for other Kasner exponents.

4.2 Non-zero center of mass momentum

If one starts with a non-vanishing center of mass momentum, π_z, at $t = -t_0$, and if the orbifold rapidity θ_0 is not negligible with respect to π_z, then one cannot drop its contribution in the Hamiltonian (25). The Wheeler-de Witt equation associated with the Hamiltonian (25) can be solved numerically, again yielding a regular solution, in particular at $t = 0$, which is very similar to the $\pi_0 = 0$ case shown in Fig. 4. Furthermore, to describe the $t > 0$ behavior, we can once again use the harmonic oscillator basis as an ansatz, but with a frequency which now depends on both time and π_0; details are given in Appendix A. Here we only summarize our findings. Asymptotically, the wave function can again be described in terms of decoupled harmonic oscillator modes, while near the singularity the straight-line

behavior (after integrating over R) remains as a characteristic feature. Thus, we can send in the vacuum state and read off the harmonic oscillator components in the outgoing solution, to find the Bogoliubov coefficients for such a transition.

From the definition in equation (27), we know that the orbifold rapidity should play a role in the physical observables, via the combination $\pi_o = \theta_0^{(2\Delta p+s)/(s+2)}\pi_z$. Thus, if as mentioned above we assume $\Delta p > -s/2$, increasing the orbifold rapidity is equivalent to increasing the center of mass momentum. Now the question is: how do the Bogoliubov coefficients change due to π_0? On the one hand, we know that classically the presence of a singularity forces the loop to increase its velocity until it reaches the speed of light at $t = 0$. As we have already seen, this speeding up is achieved by exciting higher order oscillation modes. Therefore, one would naively expect that a larger π_0 should help the loop to reach the speed of light at $t = 0$ without exciting higher order modes. On the other hand, one should expect that increasing the orbifold rapidity makes the orbifold collision more violent, thus increasing particle production. These two effects compete against each other and indeed, we see both of them at different scales. For small π_0, particle production is suppressed exponentially as $\exp(-c_1\pi_0^2 - c_2 n^{3/4})$, where $c_1 > 0$ and $c_2 > 0$ depend on the Kasner exponents, and c_2 has a mild dependence on π_0. However, for larger π_0 particle production grows as a powerlaw of π_0, while exponentially decreases with n. This powerlaw growth is in agreement with the instanton calculation of [10], where it was found that $\langle 0|\hat{N}_0|0\rangle_{out} \propto \theta_0^{(d-1)/3}$ for a $(d+1)$-dimensional spacetime. In agreement, we find for the case $d = 4$; three spatial dimensions corresponding to the effective space in which the loop oscillates plus the M-theory dimension. Figure Fig. 8 shows how particle production decays with n, and Fig. 9 depicts how the particle number of the ground level, $\langle 0|\hat{N}_0|0\rangle_{out}$, changes with π_0. At first sight, it may be worrying to think that the particle production diverges for large π_0, but actually one should have in mind that the orbifold rapidity should be small, in order to have modes created well inside the comoving Hubble horizon where the adiabatic regime can be trusted [10, 13]. Furthermore, the transverse velocity of any loop cannot be the speed of light, otherwise it could not oscillate in the xy plane.

For a gas of loops, the average velocity should be close to $1/\sqrt{2}$, as shown in [19] for flat space[4]. We can then imagine a single loop with such a velocity at $t = -t_s$ (see equation (19)), and calculate the corresponding value of π_0 using the first equation in (16) and (27). Assuming the loop is initially static ($\dot{R}(-t_s) = 0$) and of unit size ($R(-t_s) = 1$), one obtains

$$\pi_0 = \frac{v\theta_0^{(2\Delta p+2)/(s+2)}}{\sqrt{1-v^2}}. \tag{52}$$

If θ_0 is small and the velocity dispersion around the mean value is not large, then the particle production should be small. For example, for $\theta_0 \sim 1/5$ and a velocity dispersion of around ± 0.25 ([20]), the corresponding values of π_0 lie on the range $\epsilon \in (0.3, 1.93)$ (at $t = -t_s = -5$), which maps to the exponentially decaying region of Fig. 9.

Finally, an important check of the quantum model is to verify unitarity, which implies that the canonical commutation relationships should be preserved over time. This translates

[4]We can assume a flat background initially, since for a small θ_0 the size of the loops is small compare to the Hubble radius .

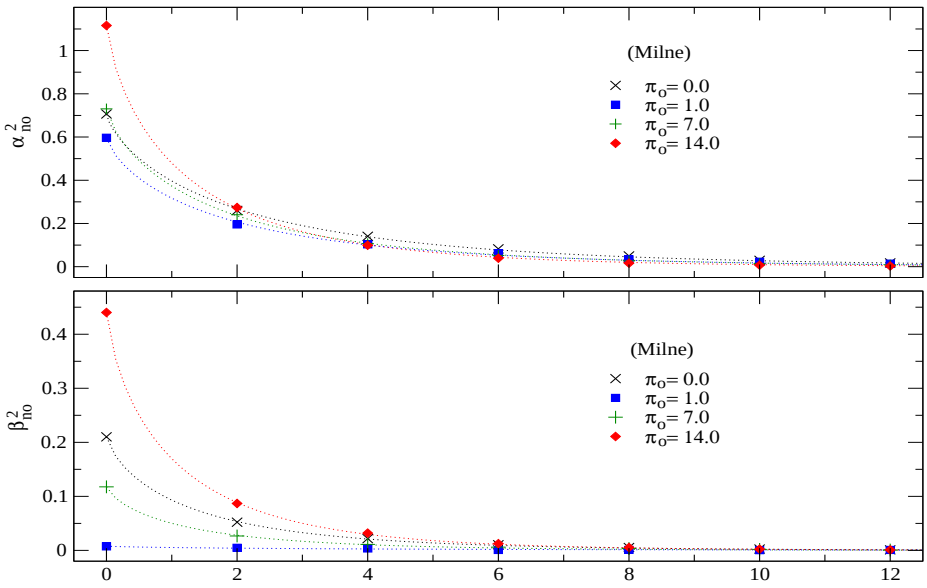

Figure 8: Bogoliubov coefficients α^2_{n0} and β^2_{n0} as functions of the mode number n for four different initial momenta, π_z, measured at $t = -t_0 = -10$. The Milne universe ($p = 0$, $p_\phi = 1$) is assumed for all cases. Fits show that both coefficients decay as $c_2 \exp(-c_1 n^{3/4})$, where c_1 has a mild dependence on π_0, but c_2 strongly depends on π_0 as shown in Figure 9.

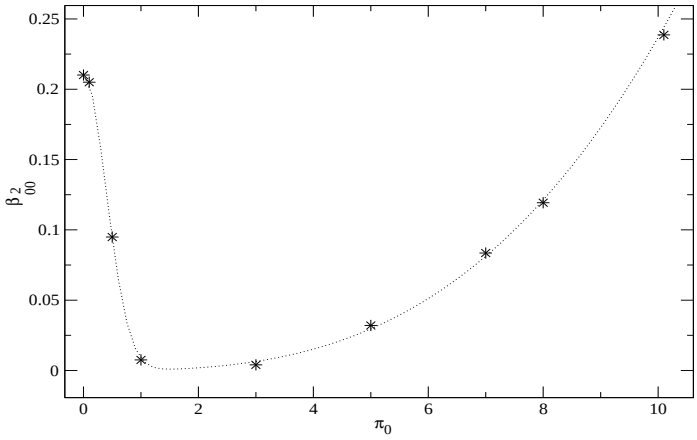

Figure 9: Bogoliubov coefficient β^2_{00} for different initial initial momentum π_0 chosen at $t_s = 5$, and assuming the Milne universe ($p = 0$, $p_\phi = 1$). For small center of mass momentum the loop needs less excited modes to reach the speed of light at $t = 0$, but a large π_0 is equivalent to a large orbifold rapidity, which increases the particle production due the more violent brane-collision. The fitting curve has a form $c_2 \exp(-c_1 \pi_0^2) + c_3 \pi_0^3$, where the c_i's are positive constants.

into the following property for the Bogoliubov coefficients

$$1 = \sum_n \alpha_{n0}\alpha^*_{n0} - \beta_{n0}\beta^*_{n0}. \tag{53}$$

One would need to sum over all states to get unity, however, one can see that using the first ten excited modes the number is close to unity (in Figure (10)).

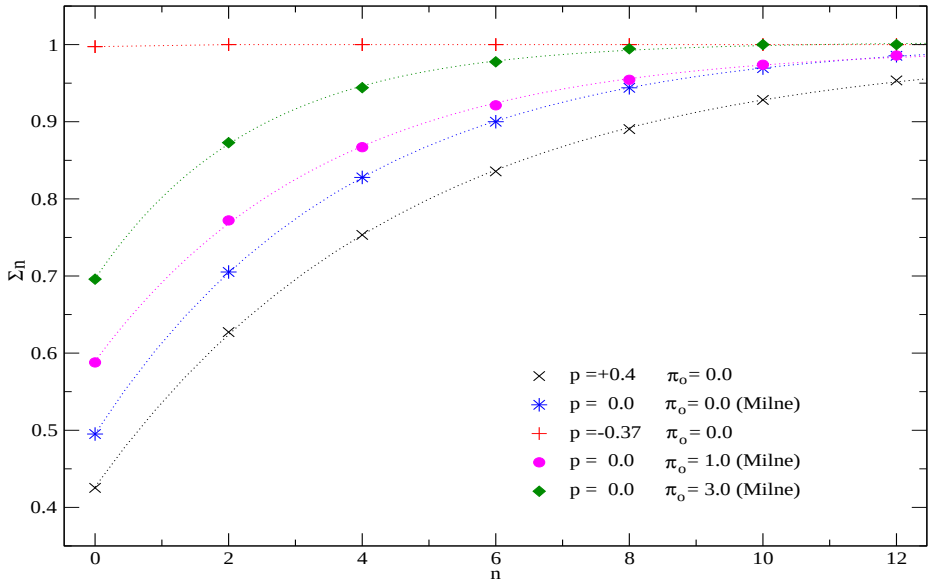

Figure 10: Plot of $\sum_n = \sum_{i=0}^{n}(\alpha_{i0}^2 - \beta_{i0}^2)$ as a function of the mode number n, for the same three Kasner metrics of Fig. 7, and for two non-zero values of π_0 at $t_s = 5$. Unitarity is preserved if $\sum_n \to 1$ as $n \to \infty$.

5 Conclusions

The nature of the big bang is one of the biggest problems facing cosmology. No one fully understands the physics that occurred in this crucial period. One of the more interesting recent proposals for the origin of the big bang, is through the collision and re-emergence of two orbifold planes in eleven dimensions [1, 2, 10]. As the two planes approach each other, the light states of the theory consist of winding M2-branes, which are described in terms of fundamental strings in a ten dimensional background. Near the brane collision region, the full eleven-dimensional metric considered is that of Euclidean space times a compactified 1+1-dimensional Milne universe. In [13], two of us considered the the classical evolution of winding membranes in such a background, showing that they suffered no blue-shift as the M theory dimension collapses, and their equations of motion remained regular across the transition from big crunch to big bang. However, one may expect there to really be small perturbations to the background metric, leading to a more general Kasner background for

the light membranes to evolve in. If this is the case, an obvious question is what happens to collapsing light M2-branes as they pass through the singularity? In this paper we have gone beyond to original classical analysis of winding membranes in [13] to include general Kasner backgrounds. By considering the corresponding Hamiltonian equations, we have been able to solve for the wave function of loops with circular symmetry and demonstrate the sensitivity of the solutions to the values of the Kasner exponents p around the Milne solution ($p = 0$ and $p_\phi = 1$). As is evident from Figures 2 and 3, although the general behavior remains similar, in particular the loop solutions remain perfectly finite, there is clear evidence that the amplitude and periodicity of the outgoing modes depend strongly on the precise value of the Kasner exponents. In the regime $p \sim -p_\phi/2$, the energy density has a mild dependence on $|t|$, and the modes do not feel the contraction or expansion of the universe, leading to no classical energy production. On the other hand, for large positive values of p, the string does feels the effects of the evolving scale factor, which produces a large effect around $t = 0$, and a greater classical production of energy. To confirm the particle interpretation of this classical result, we adopt the Wheeler-de Witt formalism to quantize the system of the evolving circular loop in the Kasner background. Circular symmetry of the loop is crucial in order to help us solve the system of equations as it allows us to assume $\partial_\sigma t = 0$, implying the time coordinate of the loop is a function of τ only. Remarkably we are able to solve the Wheeler-de Witt equation both far from and close to the singularity $t = 0$. Asymptotically, the loop is well described through a WKB approximation, given by Eqns. (33-38) in the case of very small orbifold rapidity compared to the center of mass momentum, or by Eqns. (55)-(57) for the general case. Of particular note though is the fact that near the singularity, the solution simplifies to such an extent that the integrated wave function (41) is given by a straight line in t through the singularity which allows a simple understanding of the solution on either side of $t = 0$, made evident through Figures 4 and 5. The complicated non-periodic evolution seen in Figure 4 just after the singularity provides evidence that there could well be particle production as a loop evolves through a singularity. This is confirmed in our analysis of the particle production, as seen in Figures 7 and 8 where we plot the particle production number for three separate values of the Kasner parameter including the usual Milne case, and three different center of mass momenta. In all cases, particle production is exponentially suppressed with the oscillation mode number n, and in the case of zero-center of mass momentum π_z it is independent of the orbifold rapidity θ_0. However, for a non-vanishing center of mass momentum, particle production depends on the simple function $\pi_0 = \pi_0(\theta_0, \pi_z)$, defined in (27). Production of particles is exponentially suppressed for small π_0, but has a powerlaw growth for large π_0. The two effects are expected: the first one corresponds to the fact that a small initial velocity helps the loop to reach the speed of light at the singularity without exciting higher order modes. In contrast, the second effect corresponds to the fact that a large orbifold rapidity induces a more violent big crunch/big bang, which results in more particles been produced.

As we have seen, as the loop passes through the singular point, higher order modes become light and excited, the string reaches the speed of light everywhere along it, and the effect is either an increase or decrease in the amplitude of the outgoing mode leading to classical gain or loss in energy and the production of particles whilst maintaining Unitarity.

There are of course caveats to what we have done in this paper. In reality the Kasner metric is not flat away from the singularity and thus it can receive corrections when interacting with the membrane. It is not clear how this would affect the background and subsequent analysis? Assuming we are only slightly away from Milne case, we believe that the analysis should be similar to what we have done here.

It is very encouraging that we have seen how it is possible to have finite particle production in through a singular region in a Kasner background. It is now worth seeing quite how much reheating occurs in such a scenario. An obvious, if somewhat difficult calculation is to extend this work beyond the case of a simple circular loop. Finally, it will be interesting to see how these results can be interpreted from the conformal theory description of [9].

Acknowledgements. We would like to thank Jorma Louko, Stephen Creagh, Sven Gnutzmann, Karima Righetti and Gregor Tanner for useful conversations, and also Alkistis Pourtsidou for reading the manuscript. EJC is grateful to the Royal Society, and GN is grateful to STFC for financial support.

A Non-vanishing π_0 solution

To solve the Wheeler-de Witt equation derived from the Hamiltonian (25) for a non-vanishing π_0 term, one can use the same ideas as in the $\pi_0 = 0$ case. First and to get a felling of the solution, one could study the wave equation derived from (25) for a constant time $t = t_0$, namely

$$\hat{H}\Psi = \left(\partial_t^2 - \partial_R^2 + \tilde{t}_0^{2\Delta p}\pi_0^2 + \tilde{t}_0^{2s}R^2\right)\Psi = 0, \tag{54}$$

where π_0, Δp and s are defined in (27) and (28). A solution to this equation is given again by the harmonic oscillator solution (32), but with an energy $E_n^2 = (2n+1)t_0^s + \pi_0^2 t_0^{\Delta p}$. Therefore, we can use the same ansatz (33) and the properties of the Hermite polynomials to get a recursive differential equation for the function $A_n(t)$, which is similar to (35) but with extra terms containing π_0. Actually, in the T-time variable, the A_n equation reads

$$0 = \frac{d^2A_n}{dT^2} + (1+2n)A_n + \pi_0^2\left(\frac{s+2}{2}|T|^{\frac{2}{s+2}}\right)^{2\Delta p - s} A_n + \mathcal{O}\left(\frac{1}{T}\right), \tag{55}$$

which does not have a simple analytical solution for a generic Kasner exponent combination, unlike the $\pi_0 = 0$ case. In the particular case of the Milne universe, the solution to this equation is given in terms of Whittaker functions, which are related to the polylogarithm functions. The appearance of these functions suggests a consistent description with the $1/\alpha'$-series solution of classical evolution near $t = 0$, where polylogarithm functions were found to second order in the string tension [13].

Since we are searching the asymptotic spectrum of states, it is enough to find a series solution of equation (55). The expansion parameter is $Q \equiv \pi_0^2\left(\frac{s+2}{2}|T|^{\frac{2}{s+2}}\right)^{2\Delta p - s} = \pi_0^2|t|^{2\Delta p - s}$, and the solution becomes more accurate for large $|T|$ because (14) implies $-2\Delta p + s = p_\phi + 2p_z \geq 0$. This series solution can be constructed using the ansatz

$$A_n = \exp(i\mathcal{E}_n T), \tag{56}$$

where

$$\mathcal{E}_n \equiv \mathcal{E}_n(T) = \sqrt{\beta + \alpha Q + \gamma Q^2}. \tag{57}$$

The following constants

$$\beta = 2n + 1, \qquad \alpha = \frac{s+2}{2 - s + 2\Delta p}, \qquad \gamma = 2\frac{s - 2\Delta p}{2 - s + 2\Delta p}, \tag{58}$$

solve equation (55), with an error of order $T^{-(4\Delta p+s+2)/(s+2)} \sim t^{-(4\Delta p+s+2)/2}$. So, we can use this approximate solution and calculate the particle production using the same expressions as in section 4.1.3. We assume the two vacua are given by

$$\begin{aligned} \Psi(R,t) &= \sum_n a_n^{(in)} U_n^{(in)} + (a_n^{(in)})^\dagger (U_n^{(in)})^* \qquad t \to -\infty \\ &= \sum_n a_n^{(out)} U_n^{(out)} + (a_n^{(out)})^\dagger (U_n^{(out)})^* \qquad t \to +\infty \end{aligned} \tag{59}$$

where

$$\begin{aligned} U_n^{(in)} &= \mathcal{N}_n \exp(+iE_n t) \exp(-|t|^s R^2/2) H_n(|t|^{s/2} R) \quad t < 0, \\ U_n^{(out)} &= \mathcal{N}_n \exp(-iE_n t) \exp(-|t|^s R^2/2) H_n(|t|^{s/2} R) \quad t > 0, \end{aligned} \tag{60}$$

and $E_n = \frac{2}{s+2}\mathcal{E}_n |t|^{s/2}$. The normalization factor $\mathcal{N}_n$ is given by

$$\mathcal{N}_n = \left[2^{n+1} n! \sqrt{\pi}\, (\mathcal{E}_n' T + \mathcal{E}_n)\right]^{-1/2}, \tag{61}$$

with $\mathcal{E}_n' \equiv \frac{d}{dT}\mathcal{E}_n(T)$. Therefore, by writing the vacuum solution as

$$\Psi = \mathcal{N}_0 \left[\left(a_0^{(in)} + (a_0^{(in)})^\dagger \right) \cos(E_0|t|) - i \left(a_0^{(in)} - (a_0^{(in)})^\dagger \right) \sin(E_0|t|) \right] \exp(-|t|^s R^2/2), \tag{62}$$

we can read off the outgoing solution in terms of the Bogoliubov coefficients (50), and calculate the particle production in the same way we did for the $\pi_0 = 0$ case. The results are shown in Figure 8 and summarized in Section 4.2.

References

[1] J. Khoury, B. A. Ovrut, P. J. Steinhardt and N. Turok, Phys. Rev. D **64**, 123522 (2001) [arXiv:hep-th/0103239].

[2] P. J. Steinhardt and N. Turok, Science **296**, 1436 (2002).

[3] S. Gratton, J. Khoury, P. J. Steinhardt and N. Turok, Phys. Rev. D **69**, 103505 (2004) [arXiv:astro-ph/0301395]. A. J. Tolley and N. Turok, Phys. Rev. D **66**, 106005 (2002) [arXiv:hep-th/0204091]. A. J. Tolley, N. Turok and P. J. Steinhardt, Phys. Rev. D **69**, 106005 (2004) [arXiv:hep-th/0306109]. J. Khoury, B. A. Ovrut, P. J. Steinhardt

and N. Turok, Phys. Rev. D **66**, 046005 (2002) [arXiv:hep-th/0109050]. C. Cartier, R. Durrer and E. J. Copeland, Phys. Rev. D **67**, 103517 (2003) [arXiv:hep-th/0301198]. C. Cartier, J. c. Hwang and E. J. Copeland, Phys. Rev. D **64**, 103504 (2001) [arXiv:astro-ph/0106197]. A. Cardoso and D. Wands, Phys. Rev. D **77**, 123538 (2008) [arXiv:0801.1667 [hep-th]]. K. Koyama, S. Mizuno and D. Wands, Class. Quant. Grav. **24**, 3919 (2007) [arXiv:0704.1152 [hep-th]]. E. J. Copeland and D. Wands, JCAP **0706**, 014 (2007) [arXiv:hep-th/0609183]. L. A. Boyle, P. J. Steinhardt and N. Turok, Phys. Rev. D **70**, 023504 (2004) [arXiv:hep-th/0403026]. M. Gasperini, M. Giovannini and G. Veneziano, Nucl. Phys. B **694**, 206 (2004) [arXiv:hep-th/0401112]. J. Martin and P. Peter, Phys. Rev. D **68**, 103517 (2003) [arXiv:hep-th/0307077]. M. Gasperini, M. Giovannini and G. Veneziano, Phys. Lett. B **569**, 113 (2003) [arXiv:hep-th/0306113]. M. Novello and S. E. P. Bergliaffa, Phys. Rept. **463**, 127 (2008) [arXiv:0802.1634 [astro-ph]]. R. H. Brandenberger, Phys. Rev. D **80**, 023535 (2009) [arXiv:0905.1514 [hep-th]].

[4] L. Cornalba and M. S. Costa, Phys. Rev. D **66**, 066001 (2002) [arXiv:hep-th/0203031]. V. Balasubramanian, S. F. Hassan, E. Keski-Vakkuri and A. Naqvi, Phys. Rev. D **67**, 026003 (2003) [arXiv:hep-th/0202187]. H. Liu, G. W. Moore and N. Seiberg, JHEP **0206**, 045 (2002) [arXiv:hep-th/0204168]. G. Papadopoulos, J. G. Russo and A. A. Tseytlin, Class. Quant. Grav. **20**, 969 (2003) [arXiv:hep-th/0211289]. A. Giveon, E. Rabinovici and A. Sever, Fortsch. Phys. **51**, 805 (2003) [arXiv:hep-th/0305137]. B. Craps, D. Kutasov and G. Rajesh, JHEP **0206**, 053 (2002) [arXiv:hep-th/0205101]. J. L. Karczmarek and A. Strominger, JHEP **0404**, 055 (2004) [arXiv:hep-th/0309138]. B. Craps, Class. Quant. Grav. **23**, S849 (2006) [arXiv:hep-th/0605199]. B. Craps, F. De Roo and O. Evnin, JHEP **0903**, 105 (2009) [arXiv:0812.2900 [hep-th]]. K. Madhu and K. Narayan, Phys. Rev. D **79**, 126009 (2009) [arXiv:0904.4532 [hep-th]]. K. Narayan, arXiv:0909.4731 [hep-th].

[5] J. H. She, JHEP **0601**, 002 (2006) [arXiv:hep-th/0509067]. Y. Hikida, R. R. Nayak and K. L. Panigrahi, JHEP **0509**, 023 (2005) [arXiv:hep-th/0508003].

[6] B. Pioline and M. Berkooz, JCAP **0311**, 007 (2003) [arXiv:hep-th/0307280]. M. Berkooz, B. Durin, B. Pioline and D. Reichmann, JCAP **0410**, 002 (2004) [arXiv:hep-th/0407216]. B. Durin and B. Pioline, arXiv:hep-th/0501145.

[7] B. Craps, S. Sethi and E. P. Verlinde, JHEP **0510**, 005 (2005) [arXiv:hep-th/0506180]. B. Craps, A. Rajaraman and S. Sethi, Phys. Rev. D **73**, 106005 (2006) [arXiv:hep-th/0601062].

[8] T. Hertog and G. T. Horowitz, JHEP **0407**, 073 (2004) [arXiv:hep-th/0406134]. T. Hertog and G. T. Horowitz, JHEP **0504**, 005 (2005) [arXiv:hep-th/0503071]. S. R. Das, J. Michelson, K. Narayan and S. P. Trivedi, Phys. Rev. D **74**, 026002 (2006) [arXiv:hep-th/0602107]. S. R. Das, J. Michelson, K. Narayan and S. P. Trivedi, Phys. Rev. D **75**, 026002 (2007) [arXiv:hep-th/0610053]. A. Awad, S. R. Das, K. Narayan and S. P. Trivedi, Phys. Rev. D **77**, 046008 (2008) [arXiv:0711.2994 [hep-th]]. A. Awad,

S. R. Das, S. Nampuri, K. Narayan and S. P. Trivedi, Phys. Rev. D **79**, 046004 (2009) [arXiv:0807.1517 [hep-th]]. C. S. Chu and P. M. Ho, JHEP **0604**, 013 (2006) [arXiv:hep-th/0602054]. C. S. Chu and P. M. Ho, JHEP **0802**, 058 (2008) [arXiv:0710.2640 [hep-th]]. F. L. Lin and W. Y. Wen, JHEP **0605**, 013 (2006) [arXiv:hep-th/0602124]. F. L. Lin and D. Tomino, JHEP **0703**, 118 (2007) [arXiv:hep-th/0611139].

[9] B. Craps, T. Hertog and N. Turok, arXiv:0712.4180 [hep-th]. N. Turok, B. Craps and T. Hertog, arXiv:0711.1824 [hep-th]. B. Craps, T. Hertog and N. Turok, Phys. Rev. D **80**, 086007 (2009) [arXiv:0905.0709 [hep-th]].

[10] N. Turok, M. Perry and P. J. Steinhardt, Phys. Rev. D **70**, 106004 (2004) [Erratum-ibid. D **71**, 029901 (2005)] [arXiv:hep-th/0408083].

[11] N. Ahmed and I. G. Moss, arXiv:0907.1602 [hep-th].

[12] T. Damour, M. Henneaux and H. Nicolai, Class. Quant. Grav. **20**, R145 (2003) [arXiv:hep-th/0212256].

[13] G. Niz and N. Turok, Phys. Rev. D **75**, 026001 (2007) [arXiv:hep-th/0601007].

[14] G. Niz and N. Turok, Phys. Rev. D **75**, 126004 (2007) [arXiv:0704.1727 [hep-th]].

[15] A. J. Tolley, Phys. Rev. D **73**, 123522 (2006) [arXiv:hep-th/0505158].

[16] C. M. A. Dantas, I. .A. Pedrosa and B. Baseia, Phys. Rev. A **45**, 1310 (1992).

[17] B. Craps, F. De Roo and O. Evnin, arXiv:0901.1989 [hep-th].

[18] N. D. Birrell and P. C. W. Davies, *Cambridge, Uk: Univ. Pr. 340p (1982).*

[19] A. J. Albrecht and N. Turok, Phys. Rev. D **40**, 973 (1989).

[20] R. J. Scherrer and W. H. Press, Phys. Rev. D **39**, 371 (1989).